Isotropic Magnetic Exchange Interaction through Double μ-1,2,4-Triazolato-*N*1,*N*2 Bridges: X-ray Crystal Structure, Magnetic Properties, and EPR Study of Bis(μ-3-pyridin-2-yl-1,2,4-triazolato-*N'*,*N*1,*N*2)(sulfato-*O*)aquacopper(II)diaquacopper(II) Trihydrate

Petie M. Slangen,[1a] Petra J. van Koningsbruggen,[1a] Kees Goubitz,[1b] Jaap G. Haasnoot,*[,1a] and Jan Reedijk[1a]

Leiden Institute of Chemistry, Gorlaeus Laboratories, Leiden University, P.O. Box 9502, 2300 RA Leiden, The Netherlands, and Laboratory for Crystallography, University of Amsterdam, Nieuwe Achtergracht 166, 1018 WV Amsterdam, The Netherlands

Received May 28, 1993®

The crystal and molecular structure of bis(μ-3-pyridin-2-yl-1,2,4-triazolato-*N'*,*N*1,*N*2)(sulfato-*O*)aquacopper(II)-diaquacopper(II) trihydrate ($Cu_2C_{14}H_{22}N_8O_{10}S$; $[Cu_2(pt)_2(SO_4)(H_2O)_3](H_2O)_3$ (**1**), in which pt is 3-pyridin-2-yl-1,2,4-triazolato) was determined by X-ray diffraction methods. Crystal data for **1**: $T = 298$ K, monoclinic, space group = $P2_1/a$, $a = 13.0234(5)$ Å, $b = 13.4212(6)$ Å, $c = 14.1119(4)$ Å, $\beta = 116.462(3)°$, $Z = 4$ (dinuclear molecules), and $V = 2208.2(2)$ Å^3. The least-squares refinement based on 3260 significant reflections [$I > 2.5\sigma(I)$] converged to $R = 0.045$ and $R_w = 0.068$. The structure of **1** consists of asymmetric dinuclear units, in which two symmetry independent copper(II) ions are linked by two dehydronated Hpt ligands (*i.e.*, ligands having lost H^+) bridging *via* *N*1,*N*2 in the equatorial plane. Both copper(II) ions are in a distorted square pyramidal environment, of which the basal plane around Cu2 is completed by a monodentate coordinating sulfate (Cu2–O11 = 2.000(3) Å), whereas a water molecule is coordinated to Cu1 (Cu1–O2 = 2.004(3) Å). Water molecules occupy the apical positions of both copper ions (Cu1–O1 = 2.219(5) Å, Cu2–O3 = 2.223(5) Å). The Cu1–Cu2 distance within the dinuclear unit is 4.0265(8) Å. The dinuclear units are stacked in pairs in such a way as to form tetranuclear units with a shortest Cu1–Cu2'' ($-x$, $-y$, $-z$) distance of 3.997(1) Å. The two ligand planes are above each other at a stacking distance of 3.34 Å. The magnetic susceptibility data (10–293 K) are interpreted on the basis of the spin Hamiltonian $\hat{H} = -2J(\hat{S}_{Cu1}\cdot\hat{S}_{Cu2})$, yielding $J = -49$ cm^{-1} and $g = 2.00$. The magnetic data are compared to those obtained for related double 1,2,4-triazole-*N*1,*N*2 bridged dinuclear copper(II) compounds, and magneto–structural correlations are presented for the first time for this type of dimer. The superexchange pathway involves the σ orbitals of the diazine-*N*1,*N*2 moiety of the bridging triazole network. A relation between the bridging ligand geometry (reflected in the Cu–N–N angles) and the magnitude of the magnetic interaction has been derived. The X-band powder EPR spectra, recorded at various temperatures, are typical of a triplet spin state lying above the singlet ground state.

Introduction

The magnetic properties of paramagnetic transition metal ions incorporated in various coordination compounds have been the subject of intensive study over many years.[2,3] Particular interest has been directed towards the study of dinuclear copper(II) complexes for which correlations between the singlet–triplet splitting, $2J$, and structural parameters have been made.[4] In general, several physical and structural parameters are important for understanding the magnetic properties.[2,3] The main parameters are the distance between the paramagnetic centers, the M–X–M (X = bridging ligand donor atom) angle, the extent of planarity of the bridging network, and the nature of the bridging ligand, *i.e.* in particular the electron density on the bridging group and the intrinsic properties of the anions.[2,5] Most studies deal with compounds containing two bridging monoatomic groups between the metal ions, such as hydroxo,[4,6–9] alkoxo,[10,11] chloro,[9,12–19] bromo,[15,20] fluoro,[21,22] azido,[23] and thiolato.[24,25] A successful correlation has been found for the planar dihydroxo-

* Author to whom correspondence should be addressed.
® Abstract published in *Advance ACS Abstracts*, February 1, 1994.

(1) (a) Leiden University. (b) University of Amsterdam.
(2) *Magneto-structural correlations in exchange coupled systems*; Willett, R. D., Gatteschi D., Kahn O., Eds.; NATO ASI Series No. 140; D. Reidel: Dordrecht, The Netherlands, 1984.
(3) Cairns, C. J.; Busch, D. H. *Coord. Chem. Rev.* **1986**, *69*, 1.
(4) Crawford, V. H.; Richardson, H. W.; Wasson, J. R.; Hodgson, D. J.; Hatfield, W. E. *Inorg. Chem.* **1976**, *15*, 2107.
(5) Charlot, M. F.; Kahn, O.; Chaillet, M.; Larrieu, C. *J. Am. Chem. Soc.* **1986**, *108*, 2574.
(6) Hatfield, W. E. In *Theory and Applications of Molecular Paramagnetism*; Boudreaux, E. A., Mulay, L. N., Eds.; Wiley: New York, 1976.
(7) Hodgson, D. J. *Prog. Inorg. Chem.* **1975**, *19*, 173.
(8) Hatfield, W. E. *ACS Symp. Ser.* **1974**, *No. 5*, 108.
(9) Hodgson, D. J. *J. Mol. Catal.* **1984**, *23*, 219.
(10) Mergehenn, R.; Merz, L.; Haase, W. *J. Chem. Soc., Dalton Trans.* **1980**, 1703.
(11) Merz, L.; Haase, W. *J. Chem. Soc., Dalton Trans.* **1980**, 875.
(12) Roberts, S. A.; Bloomquist, D. R.; Willett, R. D.; Dodgen, H. W. *J. Am. Chem. Soc.* **1981**, *103*, 2603.
(13) Willett, R. D.; Landee, C. P. *J. Appl. Phys.* **1981**, *52*, 2004.
(14) Livermore, J. C.; Willett, R. D.; Gaura, R. M.; Landee, C. P. *Inorg. Chem.* **1982**, *21*, 1403.
(15) O'Bannon, G.; Willett, R. D. *Inorg. Chim. Acta* **1981**, *53*, L131.
(16) van Ooijen, J. A. C.; Reedijk, J. *Inorg. Chim. Acta* **1977**, *25*, 131.
(17) Marsh, W. E.; Patel, K. C.; Hatfield, W. E.; Hodgson, D. J. *Inorg. Chem.* **1983**, *22*, 511.
(18) Roundhill, S. G. N.; Roundhill, D. M.; Bloomquist, D. R.; Landee, C. P.; Willett, R. D.; Dooley, D. M.; Gray, H. B. *Inorg. Chem.* **1979**, *18*, 831.
(19) Baran, P.; Koman, M.; Valigura, D.; Mrozinski, J. *J. Chem. Soc., Dalton Trans.* **1991**, 1385.
(20) Bloomquist, D. R.; Willett, R. D. *J. Am. Chem. Soc.* **1981**, *103*, 2615.
(21) Rietmeijer, F. J.; de Graaff, R. A. G.; Reedijk, J. *Inorg. Chem.* **1984**, *23*, 151.
(22) Velthuizen, W. C.; Haasnoot, J. G.; Kinneging, A. J.; Rietmeijer, F. J.; Reedijk, J. *J. Chem. Soc., Chem. Commun.* **1983**, 1366.
(23) Comarmond, J.; Plumeré, P.; Lehn, J. M.; Agnus, Y.; Louis, R.; Weiss, R.; Kahn, O.; Morgenstern-Badarau, I. *J. Am. Chem. Soc.* **1982**, *104*, 6330.
(24) Hatfield, W. E. *Inorg. Chem.* **1983**, *22*, 833.
(25) Hatfield, W. E. *Comments Inorg. Chem.* **1981**, *1*, 105.

0020-1669/94/1333-1121$04.50/0

bridged copper(II) compounds, where a linear relationship between the singlet–triplet splitting and the Cu–OH–Cu bridging angle exists.[4] These investigations have resulted in important insights into the superexchange mechanism propagated *via* double monoatomic bridges.

The next step forward in understanding the magnetic exchange phenomenon would be the study of double diatomic bridges. For this purpose polyfunctional ligands containing the diazine moiety, such as pyrazole,[26-30] phthalazine,[31] pyridazine,[32] and 1,2,4-triazoles,[33-35] are particularly interesting. The literature on (planar) dinuclear bis(μ-diazine)copper(II) compounds allowed Tandon *et al.* to make comparisons among the isotropic exchange transmittance capacities of various ligand systems.[31] By comparison of the six-membered heterocyclic ligands pyridazine and phthalazine, it became evident that the antiferromagnetic coupling was generally stronger *via* a pyridazine bridge than *via* a phthalazine bridge. This could be attributed to the fact that metal ion charge could be delocalized into the fused benzene ring of the phthalazine moiety.[31,36,37] When using the five-membered heterocycles, the ligand geometry has the effect of forcing the copper(II) ions to be further apart. Of these five-membered ring diazine systems, it is apparent that pyrazolate[26-30] has the capacity to propagate the antiferromagnetic exchange more efficiently than 1,2,4-triazole or 1,2,4-triazolato, which can be related to the presence of a third electronegative nitrogen atom in the triazole ring giving it the ability to polarize spins within the ring and thus limit the exchange.[31] An exception to this rule is represented by $(NBu_4)_2[Cu_2(dcp)_2]$ (dcp is 3,5-dicarboxypyrazolate).[38] Apparently, the magneto–structural correlations for different double diazine-bridged copper(II) systems are not that straightforward, and a more detailed analysis of the bridging geometry is necessary. For doubly pyrazolate-bridged copper(II) dimers, extended Hückel calculations have shown that the isotropic exchange interaction is rather insensitive to geometrical distortions such as deviations from the coplanarity of the metal ions and/or the pyrazoles.[28] So, more subtle differences in bridging ligand geometry must be invoked to account for the differences in magnetic properties observed in copper(II) compounds with closely related ligands.

Our research is directed toward the 1,2,4-triazole-bridged systems. Dinuclear copper(II) compounds containing the dichelating ligands 3,5-bis(pyridin-2-yl)-1,2,4-triazole (hereafter abbreviated as Hbpt) and 4-amino-3,5-bis(aminomethyl)-1,2,4-triazole (hereafter abbreviated as aamt) have been the subject of previous studies. In $[Cu(bpt)(CF_3SO_3)(H_2O)]_2$,[33] $[Cu(aamt)Br(H_2O)]_2Br_2(H_2O)_2CH_3OH$,[34] and $[Cu(aamt)(H_2O)_2]_2(SO_4)_2(H_2O)_4$,[35] the metal ions are linked in the equatorial coordination plane by two *via* $N1,N2$-bridging 1,2,4-triazole ligands. When the 1,2,4-triazole ligands link the metal ions in this planar and fairly symmetrical way, singlet–triplet splittings are of the order of $-2J = 194–236$ cm^{-1}. In these compounds the unpaired electron of the copper(II) ion occupies a magnetic orbital of $d(x^2-y^2)$ symmetry, which is pointing toward the coordinating triazole nitrogen atoms. Consequently, a considerable electron delocalization may take place through these nitrogens and magnetic superexchange interaction becomes possible *via* mainly the σ orbitals of the triazole ligand. Changes in the bridging geometry of the ligand are therefore likely to directly influence the efficiency of the exchange pathway.

In this paper, we describe the magnetic properties and the X-ray crystal structure of a dinuclear copper(II) complex containing a double 1,2,4-triazole-$N1,N2$ bridge of the dehydronated (*i.e.*, the ligand having lost H^+) 3-pyridin-2-yl-1,2,4-triazole (neutral ligand is abbreviated as Hpt; the coordination properties of Hpt were first studied by Hage *et al.* with Fe(II)[39] and Ru(II)[40]) in an unusual and asymmetric coordination mode. Attempts are made to establish magneto–structural correlations for copper(II) clusters containing these extended double 1,2,4-triazole-$N1,N2$ bridges.

Experimental Section

Materials. Starting Materials. Commercially available solvents and copper(II) sulfate pentahydrate were used without further purification. The ligand Hpt was synthesized according to the method of Hage[39-41] from 2-cyanopyridine (Fluka AG), hydrazine hydrate (Janssen Chimica), and formic acid (J. T. Baker) as starting materials.

Synthesis of $[Cu_2(pt)_2(SO_4)(H_2O)_3](H_2O)_3$ (1). A 2-mmol amount (0.27 g) of Hpt dissolved in a hot mixture of 10 mL of ethanol and 20 mL of water was added to 6 mmol (1.45 g) of $CuSO_4 \cdot 5H_2O$ in 10 mL of water. The hot solution was filtered, and after a few days the blue compound crystallized upon slow evaporation of the solvent at room temperature. Yield = 55%. Anal. Calc for $Cu_2C_{14}H_{22}N_8O_{10}S$: Cu, 20.45; C, 27.05; H, 3.57; N, 18.03. Found: Cu, 20.37; C, 26.96; H, 3.20; N, 18.25.

Elemental Analyses. C, H, N, and Cu determinations were performed by the Microanalytical Laboratory of University College, Dublin, Ireland.

IR and Electronic Spectra. Infrared spectra have been recorded as KBr pellets in the range 4000–250 cm^{-1} on a Perkin-Elmer 580B spectrophotometer. UV/visible spectra were obtained on a Perkin-Elmer 330 spectrophotometer using the diffuse reflectance technique with MgO as a reference.

EPR Spectra. X-band powder EPR spectra (variable temperatures down to 20 K) have been obtained on a Jeol RE2x electron spin resonance spectrometer using an ESR900 continuous-flow cryostat.

Magnetic Measurements. Magnetic susceptibilities were measured in the temperature range 10–293 K with a fully automated Manics DSM-8 susceptometer equipped with a TBT continuous-flow cryostat and a Drusch EAF 16 NC electromagnet operating at ca. 1.4 T. Data were corrected for magnetization of the sample holder and for diamagnetic contributions, which were estimated from the Pascal constants. Magnetic data were fitted to theoretical expressions by means of a Simplex routine.[42] All parameters (J, g, and p, the amount of paramagnetic impurity) were varied independently during the fitting procedure. This routine minimizes the function $R = [\sum|\chi_{obs} - \chi_{calc}|^2/\sum\chi_{obs}^2]^{1/2}$.

Crystallographic Data Collection and Refinement of the Structure. The structure of compound **1** has been solved by X-ray diffraction at 298 K. Parameters of data collection and refinement are given in Table 1. A clear blue, block-shaped crystal of approximate dimensions 0.13 × 0.13 × 0.15 mm was used for data collection on an Enraf-Nonius CAD-4 four-circle diffractometer with graphite-monochromated Cu Kα radiation (λ = 1.5418 Å) and an ω–2θ scan. A total of 4172 unique reflections were measured within the range $0 \le h \le 15$, $0 \le k \le 16$, and $-17 \le l \le 15$. Of these, 3260 were above the significance level of $2.5\sigma(I)$. The maximum value of $(\sin\theta)/\lambda$ was 0.61 Å^{-1}. Two reference reflections, (020) and (111), were measured hourly and showed an 18% intensity

(26) Pons, J.; López, X.; Casabó, J.; Teixidor, F.; Caubet, A.; Rius, J.; Miravitlles, C. *Inorg. Chim. Acta* **1992**, *195*, 61.
(27) Kamiusuki, T.; Ōkawa, H.; Inoue, K.; Matsumoto, N.; Kodera, M.; Kida, S. *J. Coord. Chem.* **1991**, *23*, 201.
(28) Ajò, D.; Bencini, A.; Mani, F. *Inorg. Chem.* **1988**, *27*, 2437.
(29) Drew, M. G. B.; Yates, P. C.; Esho, F. S.; Trocha-Grimshaw, J.; Lavery, A.; McKillop, K. P.; Nelson, S. M.; Nelson, J. *J. Chem. Soc., Dalton Trans.* **1988**, 2995.
(30) Kamiusuki, T.; Ōkawa, H.; Matsumoto, N.; Kida, S. *J. Chem. Soc., Dalton Trans.* **1990**, 195.
(31) Tandon, S. S.; Thompson, L. K.; Hynes, R. C. *Inorg. Chem.* **1992**, *31*, 2210.
(32) Abraham, F.; Lagrenee, M.; Sueur, S.; Mernari, B.; Bremard, C. *J. Chem. Soc., Dalton Trans.* **1991**, 1443.
(33) Prins, R.; Birker, P. J. M. W. L.; Haasnoot, J. G.; Verschoor, G. C.; Reedijk, J. *Inorg. Chem.* **1985**, *24*, 4128.
(34) Koomen-van Oudenniel, W. M. E.; de Graaff, R. A. G.; Haasnoot, J. G.; Prins, R.; Reedijk, J. *Inorg. Chem.* **1989**, *28*, 1128.
(35) van Koningsbruggen, P. J.; Haasnoot, J. G.; de Graaff, R. A. G.; Reedijk, J.; Slingerland, S. *Acta Crystallogr.* **1992**, *C48*, 1923.
(36) Thompson, L. K.; Lee, F. L.; Gabe, E. J. *Inorg. Chem.* **1988**, *27*, 39.
(37) Thompson, L. K.; Mandal, S. K.; Charland, J. P.; Gabe, E. J. *Can. J. Chem.* **1988**, *66*, 348.
(38) Bayoñ, J. C.; Esteban, P.; Net, G.; Rasmussen, P. G.; Baker, K. N.; Hahn, C. W.; Gumz, M. M. *Inorg. Chem.* **1991**, *30*, 2572.
(39) Hage, R.; Prins, R.; Haasnoot, J. G.; Reedijk, J.; Vos, J. G. *J. Chem. Soc., Dalton Trans.* **1987**, 1389.
(40) Buchanan, B. E.; Wang, R.; Vos, J. G.; Hage, R.; Haasnoot, J. G.; Reedijk, J. *Inorg. Chem.* **1990**, *29*, 3263.
(41) Hage, R. Ph.D. Thesis, State University of Leiden, 1991.
(42) Nelder, J. A.; Mead, R. *Comput. J.* **1965**, *7*, 308.

Table 1. Crystal Data and Details of the Structure Determination for $[Cu_2(pt)_2(SO_4)(H_2O)_3](H_2O)_3$

chem formula	$Cu_2C_{14}H_{22}N_8O_{10}S$
M_r	621.53
space group	$P2_1/a$
T, K	298
a, Å	13.0234(5)
b, Å	13.4212(6)
c, Å	14.1119(4)
$\alpha = \gamma$, deg	90
β, deg	116.462(3)
V, Å^3	2208.2(2)
Z	4 (dinuclear units)
obsd density, g·cm^{-3}	1.90
calcd density, g·cm^{-3}	1.87
θ range, deg	2.5–70
λ, Å	1.5418 (Cu Kα)
μ, cm^{-1}	38.5
final R^a	0.045
final $R_w{}^a$	0.068

^{a} $R = [\sum(|F_o| - |F_c|)/\sum|F_o|]$; $R_w = [\sum w(|F_o| - |F_c|)^2/\sum w|F_o|^2]^{1/2}$.

decrease during the 47-h collecting time. Unit-cell parameters were refined by a least-squares fitting procedure using 23 reflections with $80 < 2\theta < 86°$. Corrections for the aforementioned decay, Lorentz, and polarization effects were applied. The positions of Cu and S were found by direct methods. The remainder of the non-hydrogen atoms were found in a subsequent ΔF synthesis. The hydrogen atoms of the pyridyl group were placed in calculated positions, restrained in such a way that the distance to their carrier atom remained constant at approximately 1.09 Å, and were positionally refined. Full-matrix least-squares refinement on F, anisotropic for the non-hydrogen atoms and isotropic for the hydrogen atoms, converged to $R = 0.045$, $R_w = 0.068$, and $(\Delta/\sigma)_{max} = 0.58$. No attempt was made to determine the positions of the hydrogen atoms belonging to the water molecules. A weighting scheme $w = (10.3 + F_o) + 0.0056F_o^2)^{-1}$ was used. An empirical absorption correction (DIFABS)[43] was applied, with relative coefficients in the range of 0.88–1.89. The secondary isotropic extinction coefficient[44] refined to $G = 0.09(1)$. A final difference Fourier map revealed a residual electron density between −0.8 and 0.8 e Å^{-3} located near the sulfate anion, indicating some positional disorder. Scattering factors were taken from ref 45. The anomalous scattering of Cu and S was taken into account. All calculations were performed with XTAL,[46] unless stated otherwise. The illustrations were drawn with ORTEP.[47] Atomic coordinates and isotropic thermal parameters are found in Table 2.

Results

Description of the Structure of 1. The molecular structure and the atomic numbering of the double dinuclear copper(II) cluster are depicted in Figure 1, whereas relevant bond length and bond angle information is given in Tables 3 and 4. The monoclinic unit cell contains four asymmetric dinuclear copper(II) units and twelve lattice water molecules. The dinuclear unit consists of two copper(II) ions linked together by the two dehydronated Hpt ligands. The resulting pt anion acts as a planar dinucleating ligand with N1 and N2 as bridging atoms between the copper(II) ions, which is a well-known coordination mode for copper(II) coordination compounds.[33-35] The Cu–N(pyridine) distances are significantly larger than the Cu–N(triazole) distances. The Cu1–Cu2 distance within the dinuclear unit is 4.0265(8) Å. Two crystallographically independent, distorted square pyramidal coordinated copper(II) atoms, which differ in equatorial coordination, are present in this structure. The basal plane of the coordination pyramid around Cu1 is formed by three donor atoms of the anionic pt ligand (Cu1–N1′ = 1.961(4) Å, Cu1–N2 = 1.984(4) Å, Cu1–N31 = 2.047(4) Å) and a coordinated water molecule (Cu1–O2 = 2.004(3) Å). Cu1 lies 0.157(1) Å above the plane through its equatorial coordination sphere and is directed to the water molecule in the apical position at a distance Cu1–O1 = 2.219(5) Å. The pt ligand is coordinated to Cu2 in a similar fashion, although with somewhat different bond lengths (Cu2–N1 = 1.962(4) Å, Cu2–N2′ = 2.006(4) Å, Cu2–N31′ = 2.054(4) Å). A monodentate sulfate binds at an equatorial position with Cu2–O11 = 2.000(3) Å. Cu2 lies 0.264(1) Å above the equatorial coordination plane and is also directed toward the apical water molecule (Cu2–O3 = 2.223(5) Å).

Table 2. Final Coordinates and Equivalent Isotropic Thermal Parameters (Å^2) of the Non-Hydrogen Atoms of $[Cu_2(pt)_2(SO_4)(H_2O)_3](H_2O)_3$ with Estimated Standard Deviations in Parentheses

atom	x/a	y/b	z/c	$U_{eq}{}^a$
Cu1	0.75108(6)	0.56171(5)	0.32787(5)	0.0160(4)
S	1.0559(1)	0.36244(8)	0.82531(8)	0.0178(5)
C3	0.8014(4)	0.3607(3)	0.3781(4)	0.017(2)
C5	0.9002(4)	0.3316(4)	0.5388(4)	0.020(2)
C31	0.7308(4)	0.3568(3)	0.2634(3)	0.016(2)
C32	0.6980(4)	0.2696(4)	0.2052(4)	0.022(2)
C33	0.6345(4)	0.2775(4)	0.0960(4)	0.028(3)
C34	0.6072(5)	0.3712(5)	0.0508(4)	0.032(3)
C35	0.6420(5)	0.4541(4)	0.1141(4)	0.027(3)
N1	0.8911(3)	0.4309(3)	0.5304(3)	0.017(2)
N2	0.8263(3)	0.4489(3)	0.4252(3)	0.016(2)
N4	0.8457(3)	0.2834(3)	0.4460(3)	0.020(2)
N31	0.7029(3)	0.4480(3)	0.2199(3)	0.019(2)
O1	0.5882(3)	0.5515(3)	0.3416(3)	0.034(2)
O2	0.6846(3)	0.6598(3)	0.2087(3)	0.025(2)
O3	0.8017(3)	0.5135(4)	0.6859(3)	0.040(2)
O4	0.8423(4)	0.4809(4)	0.8977(3)	0.053(3)
O5	1.1214(4)	0.0975(4)	0.8119(5)	0.075(4)
O6	0.5936(3)	0.5831(3)	0.5395(3)	0.028(2)
O11	1.0554(3)	0.4363(2)	0.7457(2)	0.020(2)
O12	1.0525(5)	0.4145(3)	0.9149(3)	0.050(3)
O13	1.1602(4)	0.3038(4)	0.8599(4)	0.052(3)
O14	0.9549(4)	0.2993(4)	0.7769(4)	0.052(3)
Cu2	0.94474(5)	0.53247(5)	0.64211(5)	0.0142(3)
C3′	0.9244(4)	0.7362(3)	0.5851(4)	0.016(2)
C5′	0.8285(4)	0.7649(4)	0.4245(4)	0.023(2)
C31′	0.9954(4)	0.7391(3)	0.7005(4)	0.017(2)
C32′	1.0353(4)	0.8267(4)	0.7570(4)	0.022(2)
C33′	1.1010(4)	0.8191(4)	0.8657(4)	0.026(3)
C34′	1.1224(4)	0.7268(4)	0.9131(4)	0.028(3)
C35′	1.0786(4)	0.6418(4)	0.8508(4)	0.023(2)
N1′	0.8260(3)	0.6653(3)	0.4346(3)	0.018(2)
N2′	0.8886(3)	0.6474(3)	0.5409(3)	0.017(2)
N4′	0.8892(3)	0.8121(3)	0.5169(3)	0.022(2)
N31′	1.0166(3)	0.6487(3)	0.7454(3)	0.018(2)

^{a} $U_{eq} = {}^1/_3\sum_i\sum_j U_{ij}(as_i)(as_j)a_ia_j$.

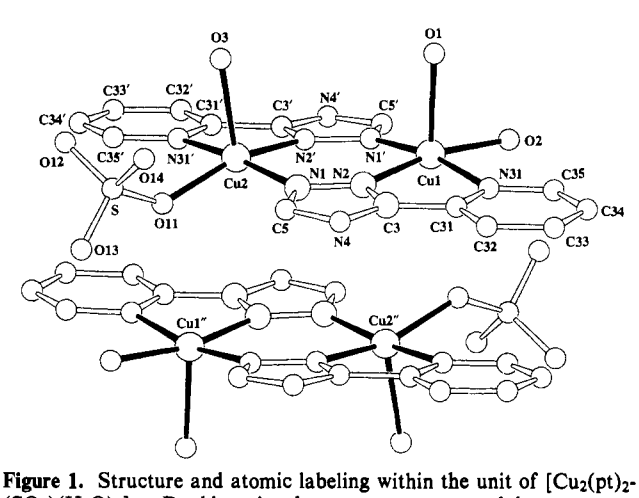

Figure 1. Structure and atomic labeling within the unit of $[Cu_2(pt)_2(SO_4)(H_2O)_3]_2$. Double primed atoms are generated by symmetry operation $-x, -y, -z$.

(43) Walker, N.; Stuart, D. *Acta Crystallogr.* **1983**, *A39*, 158.
(44) Zachariasen, W. H. *A general theory of X-ray diffraction in crystals. Acta Crystallogr.* **1967**, *A23*, 558.
(45) *International Tables for X-ray Crystallography*; Kynoch Press: Birmingham, England, 1974; Vol. IV.
(46) XTAL3.0 User's Manual. Hall, S. R., Stewart, J. M., Eds.; Universities of Western Australia and Maryland, 1990.
(47) Johnson, C. K. *ORTEP. Report ORNL-3794*; Oak Ridge National Laboratory: Oak Ridge, TN, 1965.

Table 3. Selected Bond Distances (Å) in $[Cu_2(pt)_2(SO_4)(H_2O)_3](H_2O)_3$ with Estimated Standard Deviations in Parentheses

Cu1–Cu2	4.0265(8)	C34–C35	1.370(8)
Cu1–N1′	1.961(4)	C35–N31	1.345(6)
Cu1–N2	1.984(4)	N31–C31	1.346(6)
Cu1–N31	2.047(4)	N1′–N2′	1.373(5)
Cu1–O1	2.219(5)	N2′–C3′	1.330(6)
Cu1–O2	2.004(3)	C3′–N4′	1.335(6)
Cu2–N1	1.962(4)	N4′–C5′	1.345(6)
Cu2–N2′	2.006(4)	C5′–N1′	1.345(6)
Cu2–N31′	2.054(4)	C3′–C31′	1.471(6)
Cu2–O3	2.223(5)	C31′–C32′	1.386(7)
Cu2–O11	2.000(3)	C32′–C33′	1.389(7)
N1–N2	1.364(5)	C33′–C34′	1.376(8)
N2–C3	1.326(6)	C34′–C35′	1.398(7)
C3–N4	1.354(6)	C35′–N31′	1.343(6)
N4–C5	1.345(6)	N31′–C31′	1.338(6)
C5–N1	1.338(6)	S–O11	1.496(4)
C3–C31	1.463(6)	S–O12	1.463(5)
C31–C32	1.384(7)	S–O13	1.453(5)
C32–C33	1.391(7)	S–O14	1.454(5)
C33–C34	1.383(8)		

Table 4. Bond Angles (deg) for $[Cu_2(pt)_2(SO_4)(H_2O)_3](H_2O)_3$ with Estimated Standard Deviations in Parentheses

N2–Cu1–N31	80.8(2)	N1–Cu2–O3	95.8(2)
N2–Cu1–O1	95.1(2)	N1–Cu2–O11	91.2(1)
N2–Cu1–O2	167.8(2)	N1–Cu2–N2′	94.3(2)
N2–Cu1–N1′	95.0(1)	N1–Cu2–N31′	169.8(2)
N31–Cu1–O1	91.8(2)	O3–Cu2–O11	98.2(2)
N31–Cu1–O2	89.4(1)	O3–Cu2–N2′	101.6(2)
N31–Cu1–N1′	169.3(2)	O3–Cu2–N31′	93.6(2)
O1–Cu1–O2	92.4(2)	O11–Cu2–N2′	158.7(2)
O1–Cu1–N1′	98.3(2)	O11–Cu2–N31′	91.1(1)
O2–Cu1–N1′	93.4(1)	N2′–Cu2–N31′	80.1(1)
Cu1–N1′–N2′	124.4(3)	Cu2–N1–N2	125.3(3)
Cu1–N1′–C5′	130.6(3)	Cu2–N1–C5	129.4(3)
Cu1–N2–N1	139.8(3)	Cu2–N2′–N1′	139.8(3)
Cu1–N2–C3	113.6(3)	Cu2–N2′–C3′	114.5(3)
Cu1–N31–C31	114.1(3)	Cu2–N31′–C31′	114.8(3)
Cu1–N31–C35	128.0(4)	Cu2–N31′–C35′	126.3(3)
N2–N1–C5	105.1(3)	N2′–N1′–C5′	105.0(4)
N1–N2–C3	106.4(3)	N1′–N2′–C3′	105.6(4)
N2–C3–N4	113.4(4)	N2′–C3′–N4′	114.2(4)
Cu2–O11–S	137.5(3)		
C3–N4–C5	101.2(4)	C3′–N4′–C5′	101.8(4)
N1–C5–N4	113.9(4)	N1′–C5′–N4′	113.4(4)
N2–C3–C31	118.6(4)	N2′–C3′–C31′	117.3(4)
N4–C3–C31	128.0(4)	N4′–C3′–C31′	128.5(4)
C3–C31–N31	112.4(4)	C3′–C31′–N31′	113.3(4)
C3–C31–C32	124.2(4)	C3′–C31′–C32′	123.2(4)
N31–C31–C32	123.3(4)	N31′–C31′–C32′	123.5(4)
C31–N31–C35	117.9(4)	C31′–N31′–C35′	118.8(4)
C31–C32–C33	117.9(5)	C31′–C32′–C33′	117.5(5)
C32–C33–C34	119.0(5)	C32′–C33′–C34′	119.7(5)
C33–C34–C35	119.6(5)	C33′–C34′–C35′	119.4(4)
N31–C35–C34	122.3(5)	N31′–C35′–C34′	121.1(5)
O11–S–O12	109.9(2)	O12–S–O13	110.6(3)
O11–S–O13	107.6(3)	O12–S–O14	108.3(3)
O11–S–O14	109.4(2)	O13–S–O14	110.9(3)

The basal planes of the Cu1 and Cu2 coordination pyramids make an angle of 6.5(1)°. The N2–Cu1–N31 and N2′–Cu2–N31′ bite angles are 80.8(2) and 80.1(1)°, respectively. They are comparable to the angles found for mononuclear copper(II) compounds with the related ligand 4-amino-3,5-bis(pyridin-2-yl)-1,2,4-triazole (abbreviated as abpt), *i.e.* 80.1(1)° in $[Cu(abpt)_2(H_2O)](HSO_4)_2$[48] and 80.5(2)° in $[Cu(abpt)_2(TCNQ)_2]$[49] (TCNQ is 7,7′,8,8′-tetracyanoquinodimethane). However, they are remarkably smaller than in the dinuclear $[Cu(bpt)(CF_3SO_3)(H_2O)]_2$[33] in which bite angles between 78.6(1) and 79.5(1)° were found. It is clear that when two metal ions are to be coordinated by a dichelating ligand, the bite angles are somewhat restrained; this is not the case when only one metal ion is bonded or when one of the chelating arms is missing, allowing the bite angle to be significantly larger.

Table 5. Short O–O Contacts in $[Cu_2(pt)_2(SO_4)(H_2O)_3](H_2O)_3$ with Estimated Standard Deviations in Parentheses[a]

O11–O3[1]	3.195(6)	O14–O2	2.680(7)
O11–O2[2]	3.406(5)	O1–O2[1]	3.051(7)
O12–O4[1]	2.786(8)	O1–O5	2.694(6)
O12–O4[2]	2.758(6)	O1–O6[1]	2.794(7)
O13–O5[1]	2.842(8)	O3–O4[1]	2.829(7)
O13–O2[2]	2.646(8)	O3–O6[1]	2.738(5)
O14–O3[1]	3.406(7)	O4–O5[3]	2.784(7)
O14–O5[1]	3.366(8)		

[a] Atoms with a number are generated by the following symmetry operations: (1) $^1/_2 - x, ^1/_2 + y, -z$; (2) $^1/_2 + x, ^1/_2 - y, +z$; (3) $-x, -y, -z$.

The 1,2,4-triazole bridging mode *via N1,N2* is an asymmetric one. This is reflected in the Cu1–N2–N1 and Cu2–N2′–N1′ angles, both being 139.8(3)°, and the Cu1–N1′–N2′ and Cu2–N1–N2 angles, being 124.4(3) and 125.3(3)°, respectively. This mode is clearly different from the symmetric bridging mode as observed in the aamt[34,35] and bpt compounds,[33] where all Cu–N–N angles are almost identical and are in the range 132.9(8)–135.2(2)°. Apparently, the chelate effect of the single pyridyl substituent on the triazole ring leads to this rather unusual asymmetric coordination mode.

The pyridyl group is slightly twisted with respect to the 1,2,4-triazole ring. The dihedral angle between this ring and the triazole is only 2.0(2)°. In contrast with the aamt[34,35] and bpt[33] compounds, the two ligands are not in a plane; the two least-squares planes through all atoms of these nonsymmetry-related bridging pt ligands make an angle of 6.0(1)°.

Two of these dinuclear copper(II) compounds are stacked in such a way (*via a center of symmetry*) as to form double dinuclear units with a shortest Cu1–Cu2″ (symmetry operation $-x, -y, -z$) distance of 3.997(1) Å. As a result, the present compound contains copper(II) ions that are five-coordinated, whereas usually a six coordination is found in this type of doubly-bridged triazole compounds.[33–35] This intermolecular stacking apparently prevents the coordination of a second axial ligand.

The two ligand planes lie above each other at a distance of 3.34 Å. The copper atoms are dislocated from the ligand plane in the direction of the apical water molecules, which is toward the outside of the double dinuclear cluster. This double dinuclear unit is surrounded by six lattice water molecules. The hydrogen atoms belonging to these water molecules could not be located in the crystal structure determination. Nevertheless, the short O–O contacts (see Table 5) indicate that an important hydrogen-bonding network must be stabilizing the lattice structure.

Electronic and IR Spectra. The UV/vis spectrum shows an asymmetric band centered around 13.8×10^3 cm^{-1}, which is in agreement with the presence of square pyramidal CuN_3O_2 chromophores.[50]

The IR spectrum shows evidence for the presence of a monodentate coordinated sulfate with a C_{3v} symmetry, with absorptions at 1110 (ν_3), 1040 (ν_3), 973 (ν_1), 648 (ν_4), 605 (ν_4), and 438 (ν_2) cm^{-1}.[51]

Magnetic Properties. The magnetic susceptibility has been recorded in the 10–293 K region. For **1**, the behavior of a copper(II) dinuclear compound is found with a maximum in the χ *vs* T curve at 88 K (see Figure 2). The magnetic data for compound

(48) van Koningsbruggen, P. J.; Goubitz, K.; Haasnoot, J. G.; Reedijk, J. Manuscript in preparation.
(49) Cornelissen, J. P.; van Diemen, J. H.; Groeneveld, L. R.; Haasnoot, J. G.; Spek, A. L.; Reedijk, J. *Inorg. Chem.* **1992**, *31*, 198.
(50) Hathaway, B. J.; Billing, D. E. *Coord. Chem. Rev.* **1970**, *5*, 143.
(51) Nakamoto, K. *Infrared and Raman spectra of Inorganic and Coordination Compounds*, 3rd ed.; Wiley: New York, 1978.

Table 6. Magnetic and Structural Parameters for Dinuclear Doubly Bridged Triazole-*N*1,*N*2-Copper(II) Compounds

compd[a]	J, cm^{-1}	Cu1–Cu2, Å	angles, deg: N2–Cu1–N1′ / N1–Cu2–N2′[b]	angles, deg: Cu1–N1′–N2′ / Cu2–N1–N2[b]	angles, deg: Cu1–N2–N1 / Cu2–N2′–N1′[b]	ref
$[Cu_2(pt)_2(SO_4)(H_2O)_3](H_2O)_3$	−49	4.0265(8)	95.0(1)	124.4(3)	139.8(3)	this work
			94.3(2)	125.3(3)	139.8(3)	
$[Cu(bpt)(CF_3SO_3)(H_2O)]_2$	−118	4.085(1)	90.2(1)	134.8(2)	134.9(2)	33
			90.1(1)	135.2(2)	134.5(2)	
$[Cu(aamt)Br(H_2O)]_2Br_2(H_2O)_2(CH_3OH)$	−110	4.0694(7)	92.1(1)	133.7(2)	134.2(2)	34
$[Cu(aamt)(H_2O)_2]_2(SO_4)_2(H_2O)_4$	−97	4.088(3)	91.9(4)	132.9(8)	135.1(8)	35

[a] pt = 3-pyridin-2-yl-1,2,4-triazolato; aamt = 4-amino-3,5-bis(aminomethyl)-1,2,4-triazole; bpt = 3,5-bis(pyridin-2-yl)-1,2,4-triazolato. [b] These angles are given in the second line, when the 1,2,4-triazole-*N*1,*N*2 bridges are crystallographically inequivalent.

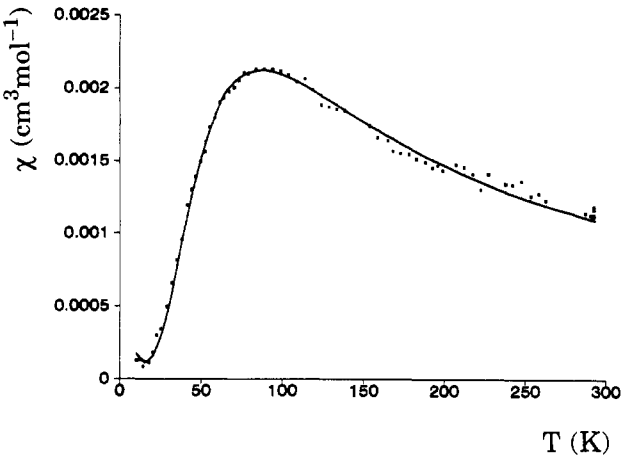

Figure 2. χ *vs* T curve for $[Cu_2(pt)_2(SO_4)(H_2O)_3](H_2O)_3$. The solid line represents the calculated curve (J = −49 cm^{-1}, g = 2.00, p = 0.5%).

1 have been fitted to the modified Bleaney and Bowers expression for the molar magnetic susceptibility for $S = {}^1/_2$ dimers.[52]

$$\chi_m = \frac{2N\beta^2g^2}{kT}[3 + \exp(-2J/kT)]^{-1}(1-p) + \chi_p p \qquad (1)$$

in which $2J$ is the singlet–triplet energy gap defined by the phenomenological spin Hamiltonian with quantum spin operators $\hat{S}_{Cu1}$ and $\hat{S}_{Cu2}$

$$\hat{H} = -2J(\hat{S}_{Cu1}\cdot\hat{S}_{Cu2}) \qquad (2)$$

In eq 1, N, g, β, k, and T have their usual meanings. The parameter p denotes the percentage of paramagnetic impurity present in the sample. A good fit has been obtained for the parameters J = −49 cm^{-1}, g = 2.00, and p = 0.5%, as is shown in Figure 2.

In this compound, the unpaired electron of the copper(II) ion is in a magnetic orbital of $d(x^2-y^2)$ symmetry, which is situated in the plane of the equatorial coordination sphere around the copper(II) ions and is partially delocalized on the equatorial ligands. The two $d(x^2-y^2)$ magnetic orbitals overlap through the 1,2,4-triazole-*N*1,*N*2 bridges. If the exchange parameter J calculated for compound **1** is compared to those of the symmetric dinuclear doubly 1,2,4-triazole-*N*1,*N*2 bridged copper(II) compounds, it is seen that in the latter case the absolute value of J is significantly larger and $2J$ is in the range of −194 to −236 cm^{-1}.[33-35] Comparison of the difference in bridging 1,2,4-triazole ligand geometry for these compounds reveals a relation between the Cu–N–N angles and the magnitude of the isotropic exchange constant. This is further illustrated by Table 6 and Figure 3. It is observed that a more symmetric bridging mode with the Cu–N–N angles close to 134° (as found in the aamt[34,35] and bpt[33] compounds) allows a larger interaction than the more asymmetric bridging mode, which is observed in the present compound. In that case, the Cu1–N2–N1 and Cu2–N2′–N1′ angles are both

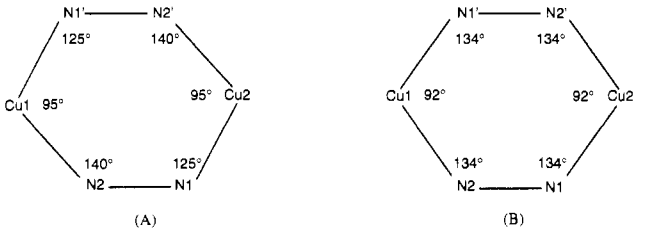

Figure 3. Schematic representation of the difference in bridging 1,2,4-triazole geometry between $[Cu_2(pt)_2(SO_4)(H_2O)_3](H_2O)_3$ (A) and the series of compounds $[Cu(aamt)(H_2O)_2]_2(SO_4)_2(H_2O)_4$, $[Cu(aamt)Br(H_2O)]_2Br_2(H_2O)_2CH_3OH$, and $[Cu(bpt)(CF_3SO_3)(H_2O)]_2$ (B).

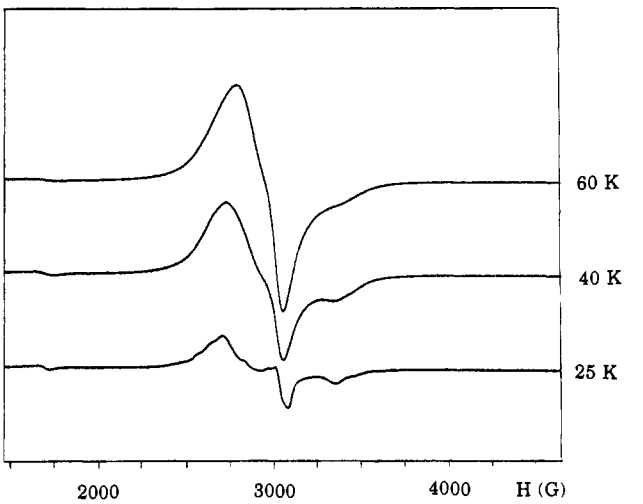

Figure 4. X-band EPR spectra of $[Cu_2(pt)_2(SO_4)(H_2O)_3](H_2O)_3$ recorded at 60, 40, and 25 K.

139.8(3)° and the Cu1–N1′–N2′ and Cu2–N1–N2 angles are 124.4(3) and 125.3(3)°, respectively. Consequently, the $d(x^2-y^2)$ orbitals situated on the Cu(II) ions in the first series of compounds are directed toward each other in such a way that the extent of overlap between them is close to maximal. So, by a symmetric 1,2,4-triazole bridging mode (in the equatorial plane) the largest possible absolute value for $2J$ is expected to be in the order of 240 cm^{-1}. A more asymmetric bridging mode will result in a less effective overlap between the $d(x^2-y^2)$ orbitals, and the isotropic magnetic exchange will decrease.

EPR Spectra. The X-band EPR spectra recorded at various temperatures are presented in Figure 4. The spectra are typical of a triplet spin state, with g = 2.14 and D = 0.09 cm^{-1}, due to the coupling of the two $S = {}^1/_2$ spins within a dinuclear unit. The antiferromagnetic coupling is clearly observed at cooling.[53] At higher temperatures, most spins are in the triplet state, which gives rise to a high intensity. The dinuclear units are too close to each other, resulting in spectra that are not very clearly resolved. At lower temperatures, most spins adopt to the singlet state which

(52) Bleaney, B.; Bowers, K. D. *Proc. R. Soc. London Ser. A* **1952**, *214*, 451.

(53) Abragam, A.; Bleaney, B. *Electron Paramagnetic Resonance of Transition Ions*; Oxford University Press: Oxford, U.K., 1970.

causes a lower intensity of the triplet spectrum; however, the dinuclear units—which are in the triplet state—become magnetically isolated and therefore the triplet spectra are better resolved. In this particular compound, the dinuclear units are stacked in such a way that a Cu(II) atom of one unit is influenced mainly by the Cu(II) atom in a second dinuclear unit at a distance of 3.997(1) Å. To observe a clearly resolved triplet spectrum, cooling to below the J temperature is necessary. This is the case at about 90 K, at which the half-field signal (with $g = 4.18$) also appears. Further lowering of the temperature results in weaker signals but better resolution.

Conclusion

The structure and magnetic properties of the first dinuclear copper(II) compound containing double 1,2,4-triazole-$N1,N2$ bridges in an asymmetric fashion have been reported.

A comparison with related Cu(II) dimers has revealed a relation between the geometry of the bridging triazole ligand and the magnitude of the isotropic magnetic exchange constant. The maximal value for $2J$ is reached when the ligand links the metal ions in the equatorial plane in the most symmetric way. In that case, the $2J$ value is expected to be in the order of -240 cm^{-1}. The absolute J-value diminishes when the bridging geometry becomes more asymmetric. At this stage it is difficult to say whether this relationship is linear with the Cu–N–N angle, as in the case of the planar dihydroxo-bridged copper(II) compounds.[4] To answer this question, further research will be directed toward other related dinuclear copper(II) compounds, which differ slightly in bridging 1,2,4-triazole ligand geometry.

This compound has an unusual structural feature of copper(II) atoms in five coordination, where only six-coordinated copper(II) ions have been observed for this type of compound. The present coordination is apparently caused by the stacking of the dimeric units, which prevents a six coordination.

Another structural difference is the presence of aqua ligands in the equatorial coordination sphere. A future study with the pt ligand will deal with the effect of changes in the equatorial coordination sphere around Cu(II) on the magnitude of the singlet–triplet splitting.[54]

Acknowledgment. The authors acknowledge the sponsoring by the Leiden Materials Science Center (Werkgroep Fundamenteel Materialen Onderzoek). Mr. J. Fraanje is thanked for the assistance with the X-ray data collection.

Supplementary Material Available: Tables SI–SVII, listing a summary of the intensity data collection, anisotropic thermal parameters, positional and thermal parameters for hydrogen atoms, bond distances and angles involving hydrogen atoms and hydrogen-bonding interactions, and selected least-squares planes, and Figure SI, showing an ORTEP projection displaying the anisotropic ellipsoids (17 pages). Ordering information is given on any current masthead page.

(54) Slangen, P. M.; van Koningsbruggen, P. J.; Haasnoot, J. G.; Jansen, J.; Gorter, S.; Reedijk, J.; Kooijman, H.; Smeets, W. J. J.; Spek, A. L. *Inorg. Chim. Acta* **1993**, *212*, 289.